

(This paper is for the Special Issue edited by
Prof. Gregoire Nicolis, Prof. Marko Robnik, Dr. Vassilis Rothos
and Dr. Haris Skokos)
**Chains of rotational tori and filamentary structures close to high
multiplicity periodic orbits in a 3D galactic potential**

M. KATSANIKAS

*Research Center for Astronomy, Academy of Athens
Soranou Efessiou 4, GR-11527 Athens, Greece*

*Section of Astrophysics, Astronomy and Mechanics,
Department of Physics, University of Athens, Greece
mkatsan@academyofathens.gr*

P.A. PATSIS

*Research Center for Astronomy, Academy of Athens
Soranou Efessiou 4, GR-11527 Athens, Greece
patsis@academyofathens.gr*

A.D. PINOTSIS

*Section of Astrophysics, Astronomy and Mechanics,
Department of Physics, University of Athens, Greece
apinots@phys.uoa.gr*

Received (to be inserted by publisher)

This paper discusses phase space structures encountered in the neighborhood of periodic orbits with high order multiplicity in a 3D autonomous Hamiltonian system with a potential of galactic type. We consider 4D spaces of section and we use the method of color and rotation [Patsis and Zachilas 1994] in order to visualize them. As examples we use the case of two orbits, one 2-periodic and one 7-periodic. We investigate the structure of multiple tori around them in the 4D surface of section and in addition we study the orbital behavior in the neighborhood of the corresponding simple unstable periodic orbits. By considering initially a few consequents in the neighborhood of the orbits in both cases we find a structure in the space of section, which is in direct correspondence with what is observed in a resonance zone of a 2D autonomous Hamiltonian system. However, in our 3D case we have instead of stability islands rotational tori, while the chaotic zone connecting the points of the unstable periodic orbit is replaced by filaments extending in 4D following a smooth color variation. For more intersections, the consequents of the orbit which started in the neighborhood of the unstable periodic orbit, diffuse in phase space and form a cloud that occupies a large volume surrounding the region containing the rotational tori. In this cloud the colors of the points are mixed. The same structures have been observed in the neighborhood of all m -periodic orbits we have examined in the system. This indicates a generic behavior.

Keywords: Chaos and Dynamical Systems, Galactic Dynamics, 4D surfaces of section

1. Introduction

Recently, Katsanikas and Patsis [2011] (hereafter KP11) studied the structure of the phase space in the neighborhood of simple periodic orbits in a 3D autonomous Hamiltonian system of galactic type. In the present paper we extend this work and we investigate the orbital behavior in the neighborhood of periodic orbits with high order multiplicity. Especially, we study the orbital behavior in the neighborhood of a stable 2-periodic and a stable 7-periodic orbit and in the neighborhood of the accompanying simple unstable periodic orbits.

In Cartesian coordinates $(x, \dot{x}, y, \dot{y}, z, \dot{z})$, if we consider our surface of section to be defined by $y = 0$, a “2-periodic” orbit is one that closes after 2 intersections with the surface of section when $\dot{y} > 0$. This is a periodic orbit of multiplicity 2. In the same way, in general, an “ m -periodic” orbit is a periodic orbit of multiplicity m . Here we study two cases with $m = 2$ and 7. For the visualization of the 4D surfaces of section we use the method of color and rotation [Patsis and Zachilas 1994]. With this method we plot the consequents in a 3D subspace of the 4D surface of section and every consequent is colored according to its location in the 4th dimension. For a description of this method, the meaning of viewing angles etc., see KP11.

Our Hamiltonian is of the form

$$H(x, y, z, \dot{x}, \dot{y}, \dot{z}) = \frac{1}{2}(\dot{x}^2 + \dot{y}^2 + \dot{z}^2) + \Phi(x, y, z) - \frac{1}{2}\Omega_b^2(x^2 + y^2) \quad (1)$$

where $\Phi(x, y, z)$ is the potential we used in our applications, i.e.:

$$\Phi(x, y, z) = -\frac{GM_1}{(x^2 + \frac{y^2}{q_a^2} + [a_1 + (\frac{z^2}{q_b^2} + b_1^2)^{1/2}]^2)^{1/2}} - \frac{GM_2}{(x^2 + \frac{y^2}{q_a^2} + [a_2 + (\frac{z^2}{q_b^2} + b_2^2)^{1/2}]^2)^{1/2}} \quad (2)$$

This potential is the same as in KP11, i.e. a triaxial double Miyamoto disk rotating around its short axis z with angular velocity $\Omega_b = 60 \text{ km s}^{-1} \text{ kpc}^{-1}$.

In our units, distance $R=1$ corresponds to 1 kpc. The velocity unit corresponds to

209.64 km/sec. For the Jacobi constant $E_j=1$ corresponds to 43950 (km/sec)^2 . For the rest of the parameters we have used the following values: $a_1 = 0 \text{ kpc}$, $b_1 = 0.495 \text{ kpc}$, $M_1 = 2.05 \times 10^{10} M_\odot$, $a_2 = 7.258 \text{ kpc}$, $b_2 = 0.520 \text{ kpc}$, $M_2 = 25.47 \times 10^{10} M_\odot$, $q_a = 1.2$, $q_b = 0.9$. The parameters q_a, q_b determine the geometry of the disks, while a, b are scaling factors.

The trajectories are calculated numerically by using a 4th order Runge-Kutta scheme, with a constant time step that secures a 13 digits precision. A typical integration for 10^4 consequents with a Core 2 Duo CPU/2.2GHz computer takes about 3.6 minutes of real time.

The calculation of the linear stability of a periodic orbit is based on the method of Broucke [1969] and Hadjidemetriou [1975]. By this method we calculate the stability indices b_1, b_2 and the quantity Δ (following the notation of Contopoulos and Magnenat [1985]). Depending on the values of the stability indices and that of Δ , a periodic orbit can be stable (S), simple unstable (U), double unstable (DU) and complex unstable (Δ). For definitions see Contopoulos and Magnenat [1985]. For a generalization of this method to systems with higher than 3 degrees of freedom see Skokos [2001].

2. Spaces of Section

2.1. Orbits

The stable and simple unstable orbits of the 2-periodic case belong to the 3D families of 2-periodic orbits “ s ” (an initially stable family) and “ u ” (an initially simple unstable family). They are bifurcations of a planar 3/1 family on the equatorial plane. The morphology of the orbits of the families s and u is depicted in Figs. 1 and 2 respectively.

We call the 3D 7-periodic families $s1$ (an initially stable family) and $u1$ (an initially simple unstable family). They are bifurcations of the family $x1v1$ [Skokos et al 2002a,b] that is associated with the vertical resonance 2/1 in our galactic system. In Figs. 3, 4 we show the morphology of the orbits of the families $s1$ and $u1$ respectively.

2.2. 4D spaces of section in the neighborhood of the 2-periodic orbits

2.2.1. Phase space structure close to s

We consider first the stable 2-periodic orbit s at $E_j = -4.33035$. We

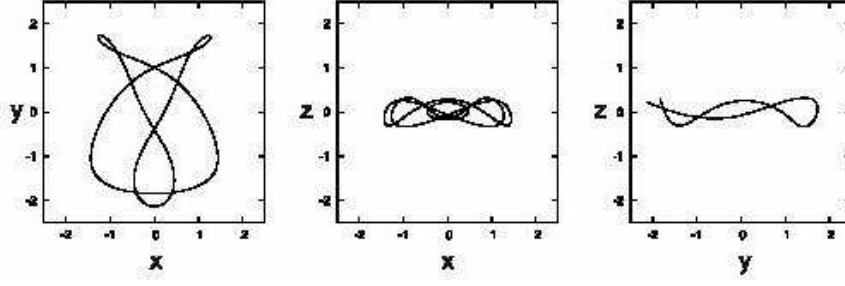


Fig. 1. Projections of a stable orbit of the 2-periodic family s at $E_j = -4.33035$.

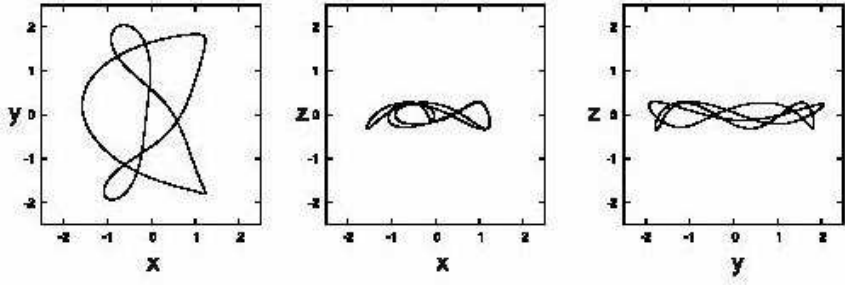


Fig. 2. Projections of a simple unstable orbit of the 2-periodic family u at $E_j = -4.33035$.

trace it at the initial conditions $(x_0, z_0, \dot{x}_0, \dot{z}_0) = (1.0867145, 0.2555081, -0.56256937, 0.049693274)$. In the neighborhood of s we observe two tori, when we perturb its initial condition x_0 , by Δx belonging to the intervals $10^{-4} \leq \Delta x \leq 4 \times 10^{-2}$ and $-10^{-4} \leq \Delta x \leq -5 \times 10^{-2}$. All these perturbations of the initial conditions are isoenergetic displacements on the surfaces of section. For example if we take $\Delta x = 4 \times 10^{-2}$ we observe two tori in Fig. 5 around the two points (black dots) of the stable 2-periodic orbit. On the two tori we observe a smooth color succession. This means that the succession of the colors of the consequents on a given structure follows the succession of the colors on the color bar at the right side of the figure. The consequents are colored according to the value of the coordinate, that is not used in the 3D spatial projection. In all diagrams of this paper the color is given according to the \dot{z} coordinate. The color values in the color bars are normalized to the $[0, 1]$ interval corresponding to $[\dot{z}_{min}, \dot{z}_{max}]$. For the details of the method the reader may refer to KP11. The smoothness of the color variation can be checked by looking at the color bar, on the right of Fig. 5, where we see that the color variation is between neighboring shades.

The colors on the upper left torus vary from red to orange to yellow and to green, while the colors on the other torus vary from green to light blue to blue. This means that the fourth value of the consequents has a smooth distribution in the 4th dimension. If we perturb the initial conditions with larger values of perturbations, for example $\Delta x = -6 \times 10^{-2}$, we observe again two tori with smooth color variation for 1000 consequents as in the previous case. However, if we continue the integration of the orbits we observe that the consequents start to deviate from two tori and they form a cloud in the 3D projection of the 4D surface of section around them (Fig. 6). In the cloud the color is mixed and this means that the points are far away in the 4th dimension. The dynamical behavior according to which an orbit stays close to an invariant torus for some time and then diffuses in phase space is typical of sticky orbits [Contopoulos and Harsoula 2008]. In Table 1 we give the values and the direction of the perturbations for which we observe tori. Just beyond this interval we encounter sticky orbits as the one in Fig. 6.

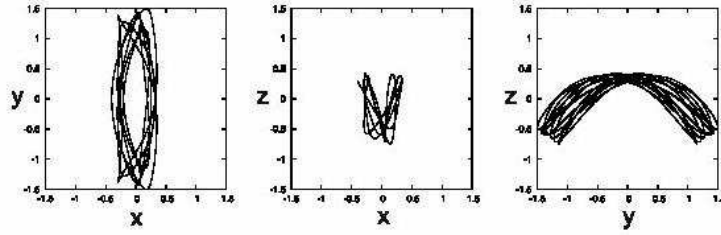


Fig. 3. Projections of a stable orbit of the 7-periodic family s_1 at $E_j = -4.622377$.

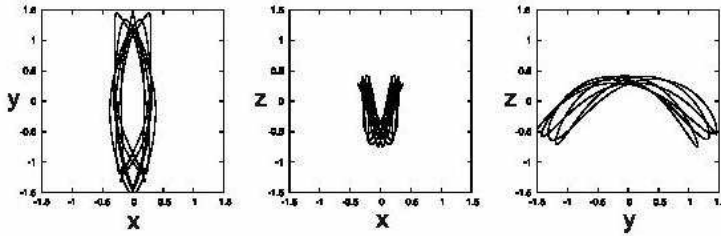


Fig. 4. Projections of a simple unstable orbit of the 7-periodic family u_1 at $E_j = -4.622377$.

2.2.2. Phase space structure close to u

Close to s , at $E_j = -4.33035$, we trace also the simple unstable 2-periodic orbit u (Fig. 5). Our code finds it at initial conditions $(x_0, z_0, \dot{x}_0, \dot{z}_0) = (0.67649546, 0.16719438, 0.78985004, 0.41351876)$. In its neighborhood we have found two types of dynamical behavior. We can see the first type if we perturb for example the initial conditions by $\Delta x = 10^{-4}$. In this case we observe in Fig. 7 a “ribbon” that connects the points of the simple unstable 2-periodic orbit. If we apply the method of color and rotation we observe in Fig. 8 a smooth color variation from red to blue. This means that the “ribbon” is a 4D structure. After 5300 intersections we observe in Fig. 9, that the consequents leave the “ribbon” and they scatter in the phase space. This orbit is also sticky in the sense that remains close to a given phase space structure for some time and then diffuses in the 4D space of section.

The second type of dynamical behavior can be seen in the neighborhood of the simple unstable 2-periodic orbit for $E_j = -4.33035$. If we add for example a perturbation in the z -direction $\Delta z = 2 \times 10^{-3}$ in the initial conditions of u we observe a filamentary surface in the 3D projection of the 4D surface of section (Fig. 10). This filamentary structure connects the points of u and forms four loops. The two of them surround the two tori that are around the

two points of s . In the regions, close to the points of u we have two self-intersections of the filamentary structure. In Fig. 10 we observe two more self-intersections indicated with arrows and the formation of 4 loops. The loops surround the periodic points s and two more points representing a periodic orbit symmetric to s with respect to the equatorial plane $z = 0$, while the arrows represent an orbit symmetric to u . The dynamics in the neighborhood of this second set of periodic orbits is similar to the one close to s and u . Now we apply the method of color and rotation in order to study the distribution of the consequents in the 4th dimension (Fig. 11). We observe, that we have also in this case a smooth color variation from red to blue and this means that the consequents are on the filamentary structure in the 4D space of section. For more than 4700 intersections the points deviate from this structure and form a cloud of points around it. Therefore in this case we encounter again the phenomenon of stickiness. Table 2 gives the range of the perturbation of the initial conditions for which we find the “ribbons” or the “filaments” connecting the points of u , for $E_j = -4.622377$. For larger values of the perturbations we find clouds of points as the one we presented in Fig. 9.

2.3. 4D spaces of section in the neighborhood of 7-periodic orbits

The structures observed close to the 2-periodic orbits, have been found in the neighborhood of every m -periodic orbit we have studied in our system. The results are qualitatively similar, but the filamentary structure that joins the points of the simple unstable orbits becomes complex as m increases. Below we give one more example of the phase space structure close to a high multiplicity orbit, this time around a 7-periodic one.

2.3.1. Phase space structure close to $s1$

We apply a perturbation both in the x -direction and z -direction in the initial conditions of the stable 7-periodic orbit of the family $s1$, $\Delta x = 1.6 \times 10^{-2}$ and $\Delta z = -5 \times 10^{-3}$, for $E_j = -4.622377$. At this Jacobi constant we find $s1$ at initial conditions $(x_0, z_0, \dot{x}_0, \dot{z}_0) = (0.25992717, 0.29991487, 0, 0)$. The perturbed orbit has been integrated for 10^4 consequents. In the (x, \dot{x}, z) 3D projection of the 4D surface of section we observe seven tori surrounding the points with the initial conditions of $s1$ (Fig. 12). In this projection we observe, that two of the tori intersect each other. To check their position in the 4th dimension we apply the method of color and rotation (Fig. 12). By taking into account the values of all tori in the 4th dimension, \dot{z} , and scaling the colors according to $[\dot{z}_{min}, \dot{z}_{max}] = [-0.617, 0.617]$, we find that to each small torus correspond one or mostly two primary colors. We observe that in the case of the two tori that intersect each other in the 3D projection (x, \dot{x}, z) we have the meeting of different colors at their intersection. This means that this intersection does not exist in the 4D space but only in the 3D projection, as expected. Next we apply the method of color and rotation only to one torus, which we call T1 and which is indicated with an arrow in Fig. 12. In Fig. 13 we observe a smooth color variation on its surface, which obviously corresponds to a different \dot{z} range than that in Fig. 12, and we see a succession of colors from red to orange, to yellow, to green, to light blue, to blue and finally to violet. Comparing this result with this found in KP11 we realize that we have a morphology typical for rotational tori [Vrahatis et al 1997, KP11]. The only difference is that we do not observe in the present case the transition of the color sequence from the external to the internal surface of

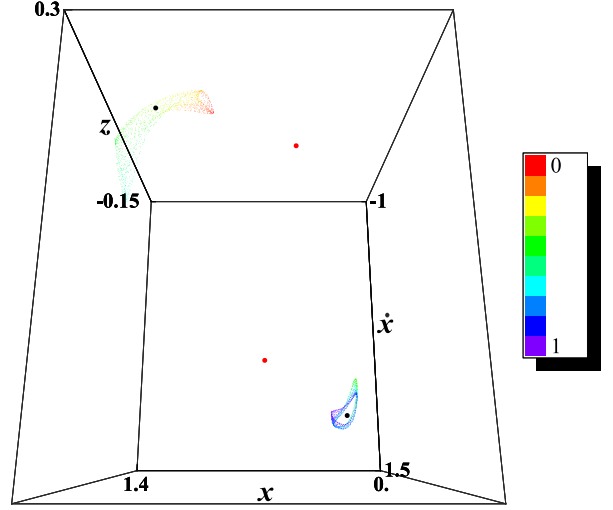


Fig. 5. The 4D surface of section for $E_j = -4.33035$ (3000 consequents) in the neighborhood of the stable 2-periodic orbit s . The initial conditions of s (black dots) are perturbed by $\Delta x = 4 \times 10^{-4}$. We use the (x, \dot{x}, z) projection to depict the consequents and the \dot{z} value ($-0.253 \leq \dot{z} \leq 0.708$) to color them. We give also the initial conditions of the associated simple unstable 2-periodic orbit u with red dots. Our point of view in spherical coordinates is $(\theta, \phi) = (22.5^\circ, 0^\circ)$.

the torus, as observed in cases around stable simple periodic orbits in KP11 (compare with figure 11 in KP11).

If we perturb the initial conditions of the periodic orbit of $s1$ by $\Delta x = 10^{-2}$ we see in Fig. 14 seven tori without any intersection of these tori in the 3D subspace. These tori have also a smooth color variation (Fig. 14). In Table 3 we give the range of the perturbation, for which we find tori in the neighborhood of $s1$.

2.3.2. Phase space structure close to $u1$

Now we investigate the properties of orbits in the phase space in the neighborhood of the simple unstable periodic orbit $u1$. The orbit we study is at $E_j = -4.622377$ and is found with initial conditions $(x_0, z_0, \dot{x}_0, \dot{z}_0) = (0.27756296, -0.084579242, 0.29935776, 0.16982513)$. Firstly we add a perturbation in the initial conditions in the x -direction $\Delta x = 10^{-4}$. In Fig. 15 we see that the consequents that are depicted with red color double bow in the 3D projection of the 4D surface of section that surrounds the seven tori that are around the points of $s1$. If we color the consequents according to the value of their fourth dimension we see in Fig. 16 that we have a smooth color variation from red to violet but at the two intersections A and

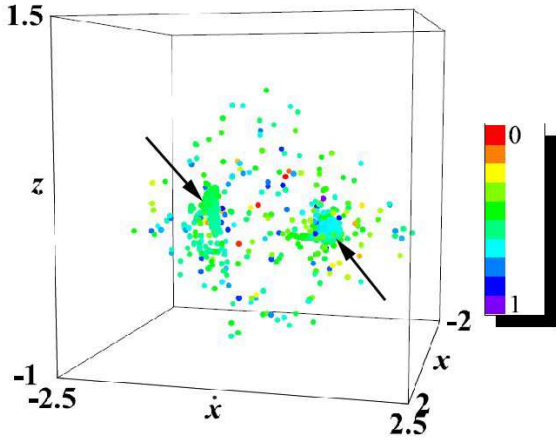


Fig. 6. 1500 consequents of the sticky orbit we found in the 4D surface of section for $E_j = -4.33035$. Color is given to the consequents according to their \dot{z} value ($-1.99 \leq \dot{z} \leq 1.982$). The orbit stays initially close to the region of the two tori (indicated with arrows) and then diffuses in phase space. We have chosen a $(\theta, \phi) = (22.5^\circ, 22.5^\circ)$ point of view for a better inspection of the regions where the consequents stay initially concentrated and the way they diffuse.

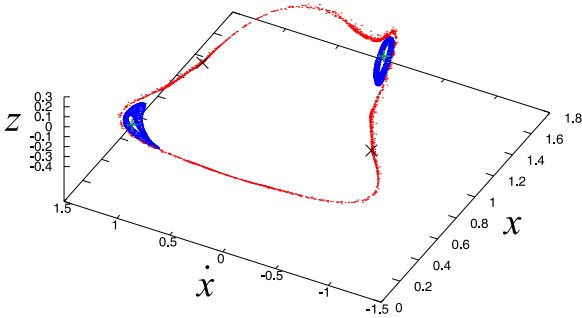


Fig. 7. The 3D subspace (x, \dot{x}, z) of the 4D surface of section for $E_j = -4.33035$ in the neighborhood of s and u . We apply a perturbation $\Delta x = 10^{-4}$ to their initial conditions and we consider 5000 consequents. The initial conditions of s are indicated with “+” in green color. We give also the initial conditions of u with \times symbols in black. Our point of view in spherical coordinates is $(\theta, \phi) = (26^\circ, 298^\circ)$. Around s a double torus structure is formed, while the perturbed orbit in the neighborhood of u forms a filamentary structure.

B we have the meeting of different colors (e.g. blue with orange). This means that we have different values of the fourth dimension at the two intersections and these intersections are only projection effects and not true intersections in the 4D space of section. The consequents depart from the structure we give in Fig. 16, after 25000 intersections.

If we perturb the same orbit by $\Delta z = -3.6 \times 10^{-4}$ at $E_j = -4.622377$. We observe in Fig. 17, that the consequents (with red) form a filamentary struc-

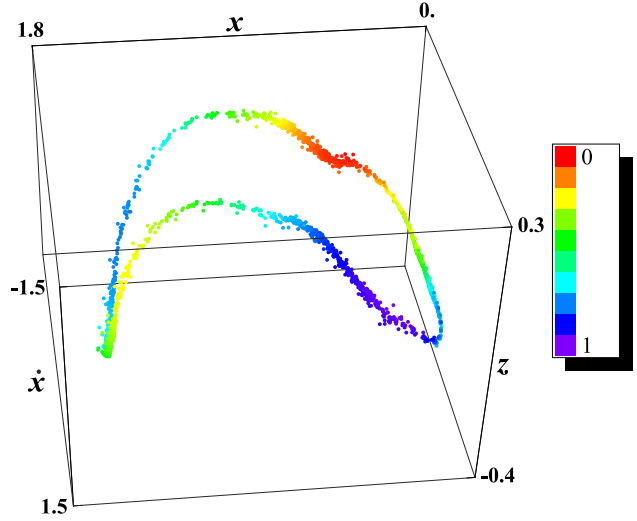


Fig. 8. The orbital behavior close to u for a deviation $\Delta x = 10^{-4}$ from its initial conditions, at $E_j = -4.33035$ (5000 intersections) in the 4D surface of section. We use the (x, \dot{x}, z) space for plotting the points and the \dot{z} value ($-0.637 \leq \dot{z} \leq 0.638$) to color them. Our point of view in spherical coordinates is given by $(\theta, \phi) = (180^\circ, 22.5^\circ)$.

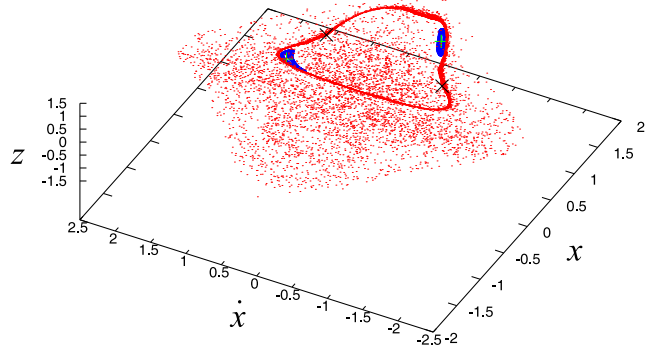


Fig. 9. A (x, \dot{x}, z) 3D projection of the 4D surface of section close to the periodic orbits s and u (\times symbol) for $E_j = -4.33035$. The “ribbon” we observe in red is the one given in 4D in Fig. 8, while the blue structures are the tori around s . This time we integrate the orbit of Fig. 8 to get 7500 (instead of 5000) consequents. We observe a cloud of points, that surrounds both the tori and the “ribbon”. Our point of view in spherical coordinates is $(\theta, \phi) = (26^\circ, 240^\circ)$.

ture that connects the points of the simple unstable 7-periodic orbit and surrounds the seven tori of the stable 7-periodic orbit. In Fig. 17 with the numbers 1 until 7 we indicate the 7 points of u_1 in the (x, \dot{x}, z) subspace. At these regions the filaments, that have been formed by evolving the orbit in time, cross each other in the 3D projection of the 4D surface of section (Fig. 17). We observe, that besides the crossings at the numbered regions, where we have the initial conditions of u_1 , we have 7 more crossings

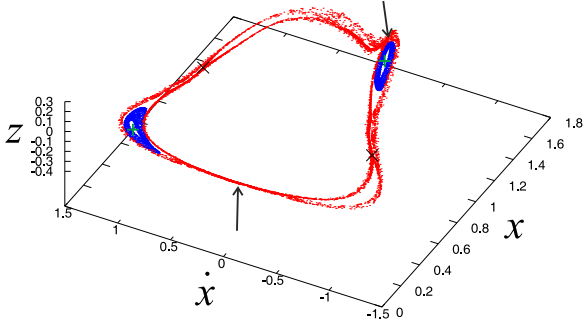


Fig. 10. The same projection as in Fig. 9, but with an orbit close to u perturbed this time in the z -direction by $\Delta z = 2 \times 10^{-3}$ (4500 consequents). This time the “ribbon” has four self-intersections in the 3D subspace. We indicate s with green “+” symbols, u with “x” in red, while the arrows point to the two additional self-intersections of the “ribbon”. Our point of view is $(\theta, \phi) = (26^\circ, 298^\circ)$.

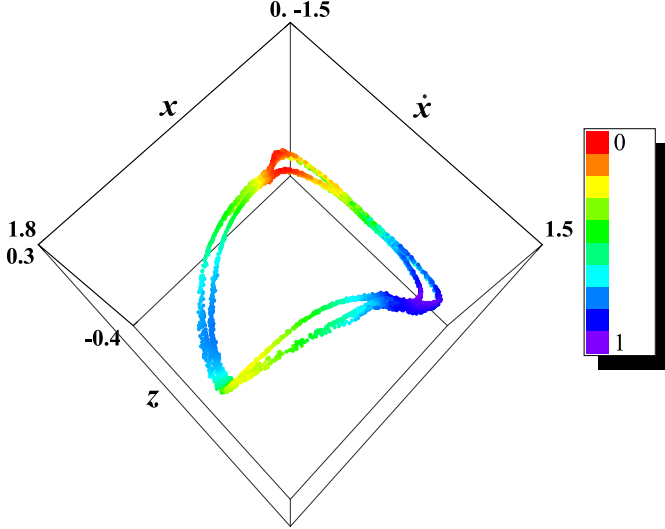


Fig. 11. The 4D representation of the “ribbon” of Fig. 10, for 4000 intersections. The consequents are colored according to their \dot{z} value ($-0.651 \leq \dot{z} \leq 0.651$). The branches of the “ribbon” that intersect themselves, have the same color at the intersections, meaning that they are true interseptions in the 4D space. Our point of view is given by $(\theta, \phi) = (22.5^\circ, 22.5^\circ)$.

of the filamentary structure by itself and the formation of 7 new loops, like those surrounding the tori around the points of $s1$. We have again here, like in the 2-periodic orbit in section 2.2.2, the presence of the symmetric family, with respect to the equatorial plane.

In Fig. 18 we observe a smooth color variation along the consequents that build the filaments. Starting from 1 we have a color succession from green to light blue, then to blue at 2, after that to light blue, then to green at 3, etc. At the regions,

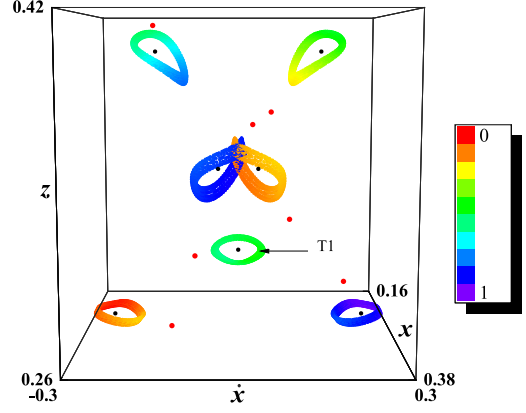


Fig. 12. The 4D surface of section for $Ej = -4.622377$ (6500 consequents) in the neighborhood of $s1$. The initial conditions of $s1$ are given with black dots. The orbit of the tori is found by perturbing the $s1$ initial conditions (see text) by $\Delta x = 1.6 \times 10^{-2}$ and $\Delta z = -5 \times 10^{-3}$. The (x, \dot{x}, z) projection is used to depict the consequents and the \dot{z} value ($-0.617 \leq \dot{z} \leq 0.617$) to color them. We give also the initial conditions of the associated simple unstable 2-periodic orbit $u1$ with red dots. Our point of view in spherical coordinates is $(\theta, \phi) = (0^\circ, 180^\circ)$. We indicate with an arrow the T1 torus, which is discussed in the text.

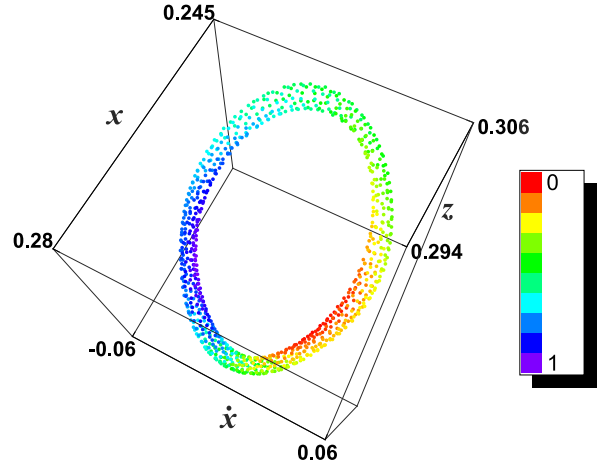


Fig. 13. Torus T1 in the 4D surface of section. Color is given to the consequents according to their \dot{z} value ($-0.092 \leq \dot{z} \leq 0.092$). We observe a smooth color variation on its surface. Our point of view in spherical coordinates is given by $(\theta, \phi) = (22.5^\circ, 45^\circ)$.

where we have the self crossing of the filaments, i.e. close to the points 1, 2, ..., 7, we observe that the regions are characterized by just one color only. For example at 1 the shade is green, at 2 blue etc. This means that the fourth coordinate \dot{z} of the consequents at these regions has this time the same value and the intersections in the 3D projections are real intersections in the 4D space. We also observe that

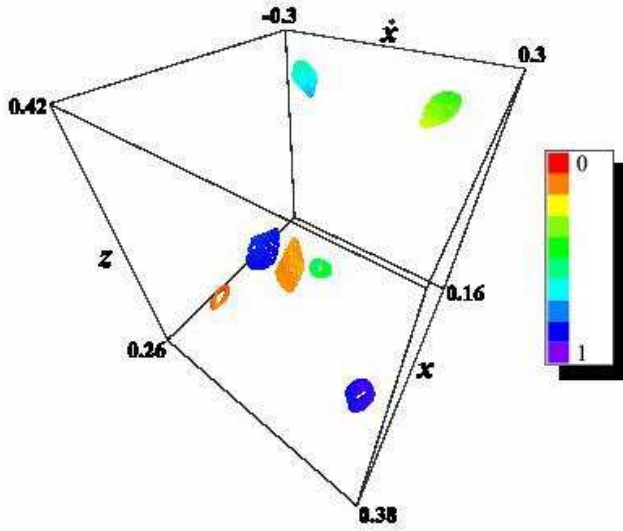


Fig. 14. Tori in the 4D surface of section for $E_j = -4.622377$ (10^4 consequents) in the neighborhood of the stable 7-periodic orbit $s1$ for $\Delta x = 10^{-2}$. Color is given to the consequents according to their \dot{z} value ($-0.592 \leq \dot{z} \leq 0.592$). Our point of view in spherical coordinates is given by $(\theta, \phi) = (22.5^\circ, 45^\circ)$.

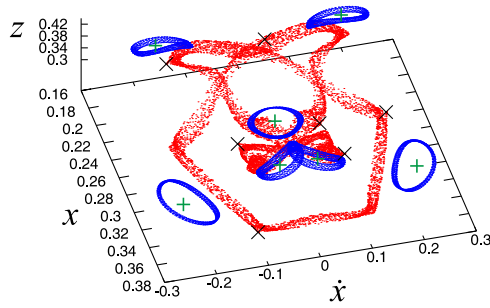


Fig. 15. The 3D (x, \dot{x}, z) projection of the 4D surface of section for $E_j = -4.622377$ at the neighborhood of $s1$ and $u1$. Both $s1$, $u1$ initial conditions have been perturbed by $\Delta x = 10^{-4}$ to get a set of seven tori and a “ribbon” structure respectively. Green “+” correspond to $s1$ and black “x” to $u1$. Our point of view in spherical coordinates is $(\theta, \phi) = (28^\circ, 48^\circ)$.

the color evolves along both branches that depart from, or arrive at the points of the unstable periodic orbit. Both branches show the same color evolution between two successive crossings.

The smooth succession of the colors along the filaments is observed as long as the consequents participate in the filamentary structure. However, if we consider more than about 6500 consequents in the

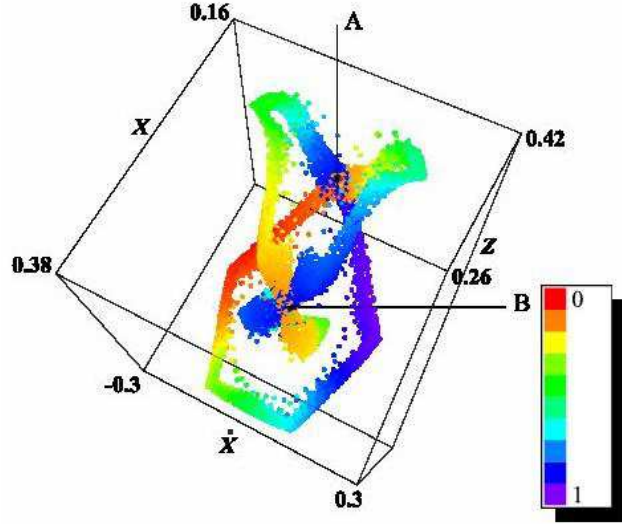


Fig. 16. The 4D surfaces of section in the neighborhood of $u1$ for the same orbit close to it depicted in Fig. 15. We consider 6000 intersections. We use the (x, \dot{x}, z) space for plotting the points and the \dot{z} value ($-0.708 \leq \dot{z} \leq 0.693$) to color them. Different colors at the intersections (at “A” and “B”) indicate that they are not true in 4D. Our point of view is $(\theta, \phi) = (22.5^\circ, 45^\circ)$.

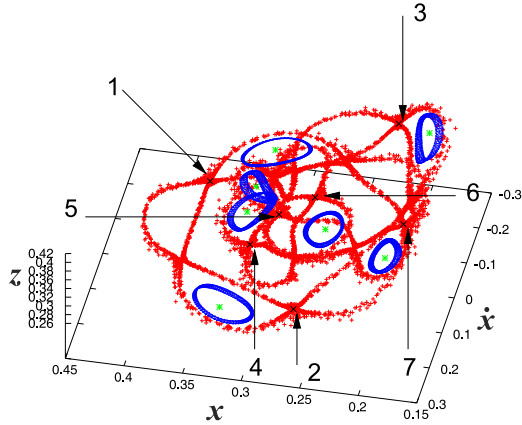


Fig. 17. The 3D (x, \dot{x}, z) projection of the 4D surface of section for $E_j = -4.622377$ at the neighborhoods of $s1$ and $u1$ for a perturbation of their initial conditions by $\Delta z = -3.6 \times 10^{-4}$. The initial conditions of $s1$ are indicated with “x” and green color and those of $u1$ with “x” black symbols. These points are numbered from 1 to 7. Our point of view in spherical coordinates is $(\theta, \phi) = (26^\circ, 192^\circ)$.

neighborhood of the $u1$ orbit, the points diffuse, occupying a large volume in the phase space and finally they form a cloud in the 3D projections that surrounds the structure we observe in Fig. 18. The dimensions of this cloud becomes about 15 times

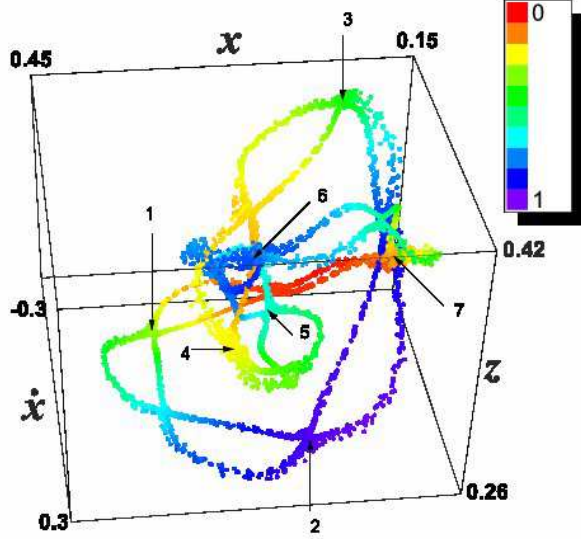


Fig. 18. The 4D representation of the orbit close to $u1$, which we give in Fig. 17, for 6000 intersections. We use the (x, \dot{x}, z) space for plotting the points and the \dot{z} value ($-0.726 \leq \dot{z} \leq 0.709$) to color them. The points 1 to 7 indicate the $u1$ initial conditions. The common colors of the branches of the filamentary structures that meet at the intersections show, that they are true intersections in 4D. Our point of view in spherical coordinates is given by $(\theta, \phi) = (180^\circ, 22.5^\circ)$.

larger in the x direction than the structure depicted in Figs. 17 and 18. This is determined by the space in which the particles are allowed to move for this Ej. The cloud of points can be seen in Fig. 19. The red configuration in the central region of the diagram is the structure we observe in Fig. 18. By giving colors to the consequents according to their distribution in the 4th dimension we have realized that in the cloud the distribution of points in the 4th dimension is mixed (Fig. 20). In Table 4 we summarize the range of perturbation for which the

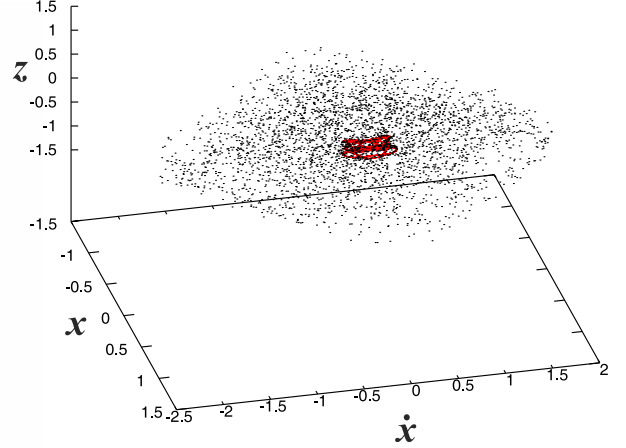


Fig. 19. The 3D (x, z, \dot{x}) projection showing a cloud of points that surrounds the orbits close to $s1$ and $u1$ presented in Figs. 17 and 18. This time we integrate the same orbit in the neighborhood of $u1$ as in the previous figures, but we consider 10000 instead of 6000 consequents. The red structure in the center of the cloud includes everything plotted in Figs. 17. Our point of view in spherical coordinates is given by $(\theta, \phi) = (37^\circ, 17^\circ)$.

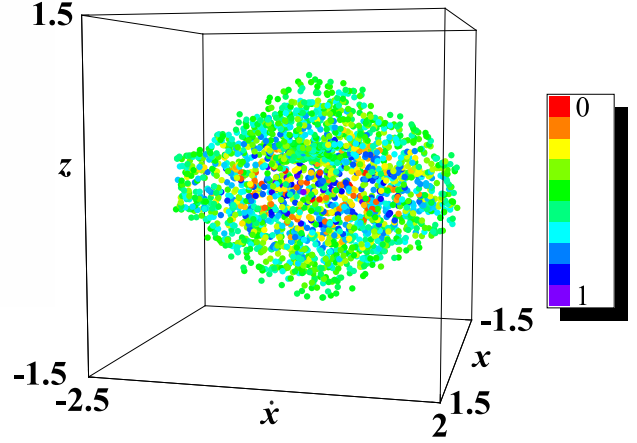


Fig. 20. The cloud of Fig. 19 in the 4D space of section. We plot 7500 consequents. We use the (x, \dot{x}, z) space for plotting the points and the \dot{z} value ($-2.29 \leq \dot{z} \leq 2.33$) to color them. We observe mixing of colors. Our point of view is $(\theta, \phi) = (180^\circ, 22.5^\circ)$.

consequents remain on the filamentary structure.

3. Lyapunov Characteristic Numbers

In this paper we study two kinds of orbits. The first kind is represented by tori in the 4D surface of section in the neighborhood of stable 2-periodic and 7-periodic orbits. The second kind is represented initially by structures confined in phase space (double bow, ribbon, “filamentary” structures etc.) and

Table 1. The intervals of the perturbations of the initial conditions of the s orbit at $E_j = -4.33035$, for which we find 4D tori around s.

Δx	$\Delta \dot{x}$	Δz	$\Delta \dot{z}$
from 10^{-4} to 4×10^{-2}	from 10^{-4} to 3×10^{-2}	from 10^{-4} to 10^{-3}	from 10^{-4} to 6×10^{-2}
from -10^{-4} to -5×10^{-2}	from -10^{-4} to -3×10^{-2}	from -10^{-4} to -10^{-3}	from -10^{-4} to -1.1×10^{-2}

Table 2. The range of perturbations in the initial conditions of u , that give ribbon or filamentary structure in the 4D surfaces of section for $E_j = -4.33035$. The first two rows correspond to the ribbons and the two last to the filaments.

Δx	$\Delta \dot{x}$	Δz	$\Delta \dot{z}$
from 10^{-4} to 3×10^{-3}	from 10^{-4} to 2×10^{-2}	from 10^{-4} to 10^{-3}	from 10^{-4} to 3×10^{-3}
from -10^{-4} to -10^{-3}	from -10^{-4} to -3×10^{-2}	from -10^{-4} to -4×10^{-3}	from -10^{-4} to -9×10^{-4}
from 4×10^{-3} to 6×10^{-2}	from 3×10^{-2} to 6×10^{-2}	from 2×10^{-3} to 10^{-2}	from 4×10^{-3} to 4×10^{-2}
from -2×10^{-3} to -5×10^{-2}	-	from -5×10^{-3} to -2×10^{-2}	from -10^{-3} to -3×10^{-2}

then by clouds in the 4D surfaces of section. These orbits are located in the neighborhood of simple unstable 2-periodic and 7-periodic orbits. In this section we calculate the “finite time” Lyapunov Characteristic Number (LCN) for these two types of orbits.

The “finite time” Lyapunov Characteristic Number is defined as:

$$LCN(t) = \frac{1}{t} \ln \left| \frac{\xi(t)}{\xi(t_0)} \right|,$$

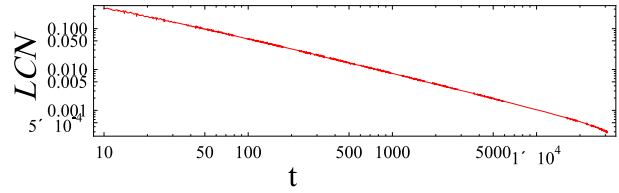
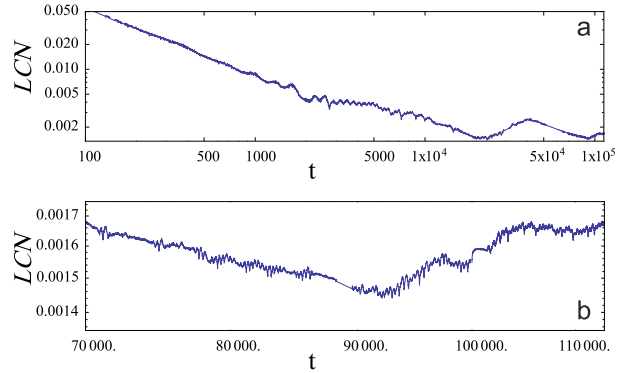
where $\xi(t_0)$ and $\xi(t)$ are the distances between two points of two nearby orbits at times $t = 0$ and t respectively (see e.g. Skokos [2010])

Firstly, for the first kind of orbits, we computed the maximal Lyapunov Characteristic Number ($mLCN$). For example, for the orbit that is represented in the 4D surface of section in Fig. 14, the value of $LCN(t)$ decreases like $1/t$ and tends to zero as we can see in Fig. 21.

Then, we calculated the “finite time” Lyapunov Characteristic Number ($LCN(t)$) for the second type of orbits, for example for the orbit in Figs. 18 and Fig. 19. In Fig. 18 we have for the first 6500 consequents a filamentary structure. During this period the $LCN(t)$ of the orbit decreases to a value 1.4×10^{-3} (Fig. 22a). Beyond that point the orbit is represented by a cloud of points in the 4D surface of section. During this phase, the $LCN(t)$ fluctuates as time increases and finally increases and tends to level off around 1.67×10^{-3} (Fig. 22b).

4. Conclusions

In this paper we studied the phase space structure in the neighborhood of stable and simple unstable periodic orbits in a rotating 3D galactic potential.

Fig. 21. The $LCN(t)$ for the orbit given in the 4D surface of section in Fig. 14. The axes are in logarithmic scale.Fig. 22. a) The evolution of $LCN(t)$ for the orbit that is presented in Figs. 18 and Fig. 19. (b) The part of Fig. 22a for $70000 \leq t \leq 115000$. The axes are in logarithmic scale.

We presented the dynamical behavior of two sets of stable-simple unstable orbits. The first was in the neighborhood of periodic orbits of multiplicity $m = 2$, and the second in the neighborhood of periodic orbits of multiplicity $m = 7$. For less than 6000 consequents we observed a direct correspondence between the standard configuration, which we encounter in a resonance zone in 2D autonomous Hamiltonian systems, and the structure of phase space in our 4D spaces of section, namely a succession of elliptic and hyperbolic points. This means

Table 3. The range of perturbations in the initial conditions of u , that give tori or tori with intersection in the 3D projections of the 4D surfaces of section for $E_j = -4.622377$. The first two rows correspond to the tori and the two last to the tori with intersection.

Δx	$\Delta \dot{x}$	Δz	$\Delta \dot{z}$
from 10^{-4} to 1.3×10^{-2}	from 10^{-4} to 3×10^{-2}	from 10^{-4} to 1.6×10^{-3}	from 10^{-4} to 10^{-1}
from -10^{-4} to -1.1×10^{-2}	from -10^{-4} to -3×10^{-2}	from -10^{-4} to -5×10^{-3}	from -10^{-4} to -10^{-1}
from 1.4×10^{-2} to 1.8×10^{-2}	from 4×10^{-2} to 6×10^{-2}	-	-
from -1.2×10^{-2} to -1.7×10^{-2}	from -4×10^{-2} to -6×10^{-2}	-	-

Table 4. The range of perturbations in the initial conditions of u , that give double bow or filamentary structure in the 4D surfaces of section for $E_j = -4.622377$. The first two rows correspond to the double bows and the two last to the filaments.

Δx	$\Delta \dot{x}$	Δz	$\Delta \dot{z}$
from 10^{-4} to 7×10^{-4}	from 10^{-4} to 3×10^{-3}	from 10^{-4} to 2×10^{-4}	from 10^{-4} to 6×10^{-3}
from -10^{-4} to -9×10^{-4}	from -10^{-4} to -6×10^{-3}	from -10^{-4} to -2×10^{-4}	from -10^{-4} to -9×10^{-3}
from 8×10^{-4} to 1.6×10^{-2}	from 4×10^{-3} to 2×10^{-2}	from 3×10^{-4} to 4×10^{-3}	from 7×10^{-3} to 10^{-1}
from -10^{-3} to -10^{-2}	from -7×10^{-3} to -8×10^{-2}	from -3×10^{-4} to -5×10^{-3}	from -10^{-2} to -10^{-1}

that also in the case we study we observed a succession of stable and *simple* unstable points in the 4D spaces of section. For larger integration times the consequents diffuse and occupy a larger volume of the phase space. We found similar behavior for all cases of m -periodic orbits we studied in this system.

The following are the main conclusions from our work:

- In the neighborhood of the stable m -periodic orbit we found m tori surrounding its initial conditions. We found smooth color variation along these tori in two ways. Along a particular torus and also along all m tori, considering them as one object. This depends on the scale of the fourth coordinate, which gives the colors to the consequents. These tori are *rotational* tori in the terminology introduced by Vrahatis et al. [1997]. Similar structures can be seen in the paper by Martinet & Magnenat [1981]. However, we did not observe in the present study the color transition from the external to the internal side of the torus on the individual tori as in some cases in KP11.
- Integrating an orbit close to a simple unstable m -periodic orbit to obtain a few thousands of consequents, we found that they form a filamentary structure with smooth color variation in the 4th dimension. The filaments that are formed in this way connect the points of the simple unstable m -periodic orbit and surround the seven tori around the points of the stable m -periodic orbit. The filamentary structures appear either as “ribbons” or as “bows” in the 4D spaces of section.
- In the regions close to the points of the simple un-

stable periodic orbit two branches of a filamentary structure meet and their consequents have the same color. This shows, that we have at these points self-intersections of the structures in the 4D space of section.

- The above described situation is a direct extrapolation of the typical case of a 2D autonomous Hamiltonian system with the chain of stability islands and the chaotic zone, which connects the points of the corresponding unstable periodic orbit. We note that in this 3D case the unstable orbit is *simple* unstable and we have a smooth color variation along the filaments when we consider the first few thousands of the intersections in the space of section.
- We encountered cases, where the consequents that remained on the filaments and reinforced this structure for a few thousand intersections, diffused later in the 4D space. The diffusion in the 4D space, was characterized by mixing of colors.

Acknowledgments We thank Prof. Contopoulos for fruitful discussions and valuable comments. MK is grateful to the “Hellenic Center of Metals Research” for its support in the frame of the current research.

5. References

Broucke R. [1969] “Periodic orbits in the elliptic restricted three-body problem” *NASA Tech. Rep.* 32-1360, 1-125.

- Contopoulos G. and Magnenat P. [1985] “Simple three-dimensional periodic orbits in a galactic-type potential” *Celest. Mech.* **37**, 387-414.
- Contopoulos G. [2002] *Order and Chaos in Dynamical Astronomy* Springer-Verlag, New York Berlin Heidelberg.
- Contopoulos G. and Harsoula M. [2008] “Stickiness in Chaos” *Int. J. Bif. Chaos* **18**, 2929-2949.
- Hadjidemetriou J.D. [1975] “The stability of periodic orbits in the three-body problem” *Celest. Mech.* **12**, 255-276.
- Katsanikas M. and Patsis P.A. [2011] “The structure of invariant tori in a 3D galactic potential” *Int. J. Bif. Chaos* (in press) (KP11).
- Martinet L. and Magnenat P. [1981] “Invariant surfaces and orbital behavior in dynamical systems with 3 degrees of freedom.” *Astron. Astrophys.* **96**, 68-77.
- Patsis P.A. and Zachilas L. [1994] “Using Color and rotation for visualizing four-dimensional Poincaré cross-sections:with applications to the orbital behavior of a three-dimensional Hamiltonian system” *Int. J. Bif. Chaos* **4**, 1399-1424.
- Skokos Ch. [2001] “On the stability of periodic orbits of high dimensional autonomous Hamiltonian Systems” *Physica D* **159**, 155-179.
- Skokos Ch., Patsis P.A. and Athanassoula E. [2002a] “Orbital dynamics of three-dimensional bars-I. The backbone of three-dimensional bars. A fiducial case” *Mon. Not. R. Astr. Soc.* **333**, 847-860.
- Skokos Ch., Patsis P.A. and Athanassoula E. [2002b] “Orbital dynamics of three-dimensional bars-II. Investigation of the parameter space” *Mon. Not. R. Astr. Soc.* **333**, 861-870.
- Skokos Ch. [2010] “The Lyapunov Characteristic Exponents and their Computation”, *Lect. Not. Phys.* **790**, 63-135.
- Vrahatis M.N., Isliker H. and Bountis T.C. [1997] “Structure and breakdown of invariant tori in a 4-D mapping model of accelerator dynamics” *Int. J. Bif. Chaos.* **7**, 2707-2722.